

## PLV/PAC Feature Extraction Units for Implantable Neural Interfaces: Review

Hoda Yassin, [HodaYassin@eng.aswu.edu.eg](mailto:HodaYassin@eng.aswu.edu.eg)

El-Sayed Hasaneen, [hasaneen@aswu.edu.eg](mailto:hasaneen@aswu.edu.eg)

Department of Electrical Engineering, Aswan University, Egypt

**Abstract:**— Neural interfaces shows promise in treating neurological conditions such as Epilepsy, Depression, and Parkinson's disease. To enable fully implantable treating interfaces, efficient oscillatory feature extraction units are required. This article explores different techniques suggested for extracting phase locking value (PLV) and phase amplitude coupling (PAC) features. Additionally, the article provides an overview of the current state-of-the-art units and highlights their limitations.

**Keywords:** — Feature extraction, oscillatory synchronization, phase locking value (PLV), phase-amplitude coupling (PAC).

### I. Introduction

In neuroscience, synchronization between brain regions is quantified with phase locking value (PLV) and phase-amplitude coupling (PAC) [1-8]. PLV is a statistic feature that measures the level of phase synchronization between two signals within the same frequency bands by a vector whose magnitude represents the level of synchronization by a value between zero and one. PLV between two signals  $S_1$  and  $S_2$  is defined as [9-11]:

$$PLV = \frac{1}{N} \sqrt{(\sum_{i=1}^N \sin \Delta \theta_i)^2 + (\sum_{i=1}^N \cos \Delta \theta_i)^2} \quad (1)$$

$$\Delta \theta_i = \theta_1 - \theta_2 \quad (2)$$

where  $N$  is the number of samples of the averaging window, and  $\theta_{1,i}$  and  $\theta_{2,i}$  are the instantaneous phases of  $S_1$  and  $S_2$  at the  $i^{th}$  sample.

Phase-amplitude coupling (PAC) is a type of cross-frequency feature in which the amplitude of a high-frequency oscillation is modulated by the phase of a low-frequency oscillation. Mean vector length (MVL) is a common measure for PAC. PAC based on the MVL is defined as [11]:

$$PAC = \frac{1}{N} \sqrt{(\sum_{i=1}^N A_{m,i} \sin \theta_{p,i})^2 + (\sum_{i=1}^N A_{m,i} \cos \theta_{p,i})^2} \quad (3)$$

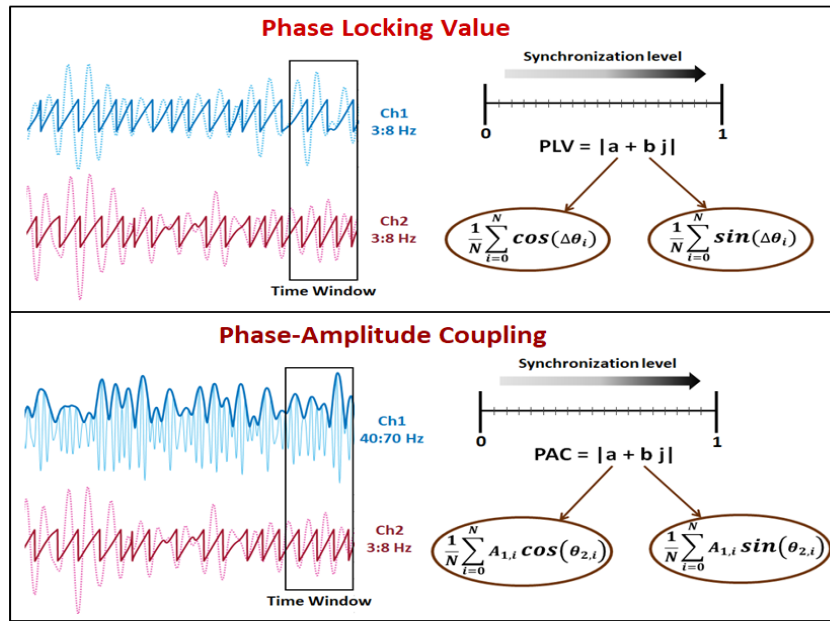


Figure 1: Phase locking value and phase-amplitude coupling features.

where  $N$  is the number of samples of the averaging window,  $\theta_{p,i}$  is the instantaneous phase of the low-frequency phase-modulating signal, and  $A_{m,i}$  is the instantaneous magnitude of the high-frequency amplitude-modulated signal, at the  $i^{th}$  sample.

A typical PLV/PAC feature extraction unit comprises two main blocks: a complex signal extractor and a PLV/PAC computation unit. The raw input data is fed into the complex signal extractor to obtain the real and imaginary components of signals within the frequency bands of interest. The PLV/PAC computation unit uses the extracted complex signals to obtain the phase and magnitude information necessary for calculating the PLV and PAC features. Various implementations of the PLV/PAC extraction unit were suggested, differing in terms of feature accuracy, hardware complexity, area occupation, and power consumption [9, 11-16]. This review article examines the state-of-the-art implementations of the PLV/PAC extraction units. Section II reviews the conventional techniques for extracting complex signals. Section III explores the commonly used PLV/PAC computation techniques. Section IV introduces a brief insight into the architectures of the PLV/PAC extraction units. The main limitations of the state-of-the-art PLV/PAC extraction units are highlighted in Section V. The conclusion is provided in Section VI.

## II. Complex Signal Extraction Techniques

Complex signal extraction involves filtering the input signal into different frequency bands and obtaining the real and imaginary components of each band. Fourier Transform (FT), ShortTime Fourier Transform (STFT), Morlet Wavelet (MWT), and Band-pass filtering followed by the Hilbert Transform (BPFH) are conventional techniques for complex signal extraction [17-19]. The techniques are discussed and compared in this section.

### A. Fourier Transform

FT extracts complex signals with single-tone resolution. The transform uses a complex sinusoidal kernel (sine and cosine). The cosine extracts the real component of the complex signal, while the sine extracts the imaginary one. FT at each frequency is equivalent to applying two single-tone filters with a 90-degree phase shift. FT assumes a stationary condition for the input signal, making it an inaccurate transform for non-stationary signals such as neural activities. However, a neural activity often remains stationary for hundreds of milliseconds. A transform

that assumes stationarity over a specific time interval can effectively extract complex signals from neural activity [19].

### B. Short-Time Fourier Transform

STFT involves computing the FT of a time window moving over the input signal [20, 21]. This is equivalent to windowing the complex sinusoidal kernel of FT. Hence, the stationarity assumption is applied only over the time window. STFT is equivalent to two band-pass filters at each frequency, with the same magnitude response and a 90-degree phase shift. The bandwidth depends on the length of the time window that reflects the time-frequency resolution. A short window has a high time resolution but poor frequency resolution, while a long window has a high frequency resolution but poor time resolution. STFT has a constant window length, resulting in a fixed frequency resolution and a trade-off between low and high-frequency accuracy. Accurate extraction across all bands requires a technique with frequency-controlled resolution.

### C. Morlet Wavelet

A wavelet is a time-limited signal with zero average [22, 23]. MWT is a type of wavelet composed of sine and cosine functions multiplied by a Gaussian window. The duration of that window varies with wavelet frequency, allowing for frequency-controlled resolution [24, 25]. The frequency response of MWT consists of two band-pass filters with the same magnitude response and a 90° phase shift. The center frequency is the same as the sinusoidal frequency, while the bandwidth depends on window duration. A set of wavelets with similar properties but different frequencies is known as a wavelet family. An example of a MWT family is shown in Fig.2.

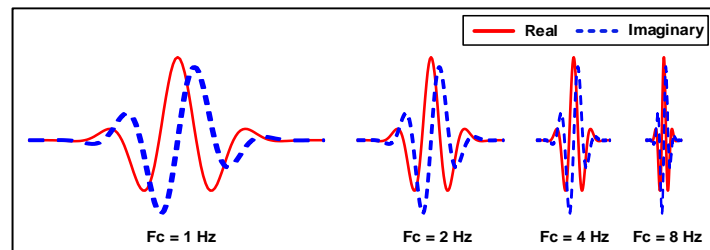


Figure 2: An example of a Morlet wavelet family.

MWT hardware implementation requires two wavelet filters for each extraction band, which leads to a significant number of taps and multipliers. Although Morlet wavelets are suitable for extracting complex signals from neural activities, their hardware complexity makes them rarely used for on-chip feature extraction.

### D. Band-Pass Filtering and Hilbert Transform

A band-pass filter bank followed by the Hilbert transform performs complex signal extraction with frequency-controlled resolution. The filter bank selects the desired frequency bands. The Hilbert transform obtains the imaginary components of the bands. This technique provides greater control over the filter characteristics compared to the Morlet wavelet convolution. Additionally, the Hilbert transform, as an all-pass filter with 90° phase shift, is suitable for being shared between multiple frequency bands. However, the required taps and multipliers are still significant. Generally, the filter-Hilbert method is the conventional technique for on-chip feature extraction [9-11, 14, 16].

### III. PLV/PAC Computation Techniques

The computation of PLV and PAC requires extracting sine and cosine values and magnitude information. The sine and cosine are typically extracted by computing the phase from the complex signals and obtaining the sine and cosine values of that phase. This two-step extraction process can be achieved using CORDIC processors [9-11] or a light phase extractor (LPE) associated with a trigonometric lookup table (LUT) [14-16]. Magnitude extraction, on the other hand, is performed using a CORDIC processor [9-11] or the L-infinity norm approximation [14-16]. This section explains the CORDIC processors algorithm, the LPE with LUT technique, and the 1-infinity norm.

#### A. CORDIC Algorithm

Coordinate Rotation Digital Computer (CORDIC) algorithm is an iterative method for computing elementary functions such as trigonometric and logarithm functions. CORDIC Algorithm involves iterations on three equations as follows [9]:

$$\begin{aligned}
 & \text{for } n = 1 : M \\
 & X[n + 1] = X[n] + Y[n] 2^{-n} \\
 & Y[n + 1] = Y[n] - \text{sign}(Y[n]) X[n] 2^{-(n-1)} \\
 & Z[n + 1] = Z[n] - \text{sign}(Y[n]) \arctan(2^{-(n-1)})
 \end{aligned} \tag{4}$$

where  $n$  is the iteration parameter, and  $M$  is the number of iterations.

To extract the phase and magnitude of a complex signal, the real and imaginary components are assigned to  $X[1]$  and  $Y[1]$ , respectively.  $Z[1]$  is set to 0. The values of  $X[M]$  and  $Z[M]$  represent the scaled magnitude and phase of the input signal, respectively. The algorithm for computing sine and cosine is similar with  $Y[1]$  set to 0,  $X[1]$  is to the CORDIC aggregate constant, and  $Z[1]$  to the phase. The value of  $X[M]$  represents the required cosine value, while  $Y[M]$  represents the sine. The iterative calculation nature of the CORDIC algorithm leads to complex hardware structure, high power consumption, and large occupation area. Achieving high accuracy requires high number of iterations, creating a complexity-accuracy trade-off. The optimal design should be studied based on the application requirements. For oscillatory feature extraction, 16 iterations may be enough, but it still results in high area and power consumption [9, 16, 18].

#### B. Light Phase Extractor and LUTs

The light phase extractor (LPE) use a linear arc-tangent approximation (LAA) to estimate the phase of an input complex signal. LAA calculates the phase from the real and imaginary components as a sum of a fractional part and an offset value. The phase extraction equations based on LAA are as follows [16]:

$$\text{Phase} = \begin{cases} 0 + \frac{IM}{4RE} & RE > 0, RE > IM \\ 0.5 - \frac{RE}{4IM} & IM > 0, IM > RE \\ \text{sign}(IM) \times 1 + \frac{IM}{4RE} & RE < 0, RE > IM \\ -0.5 - \frac{RE}{4IM} & IM < 0, IM > RE \end{cases} \tag{5}$$

where  $RE$  and  $IM$  are the real and imaginary components of the input signal.

After light phase extraction, sine and cosine values are retrieved using a trigonometric Look-Up Table (LUT). This method is much simpler and more power efficient compared to the CORDIC method, with negligible accuracy loss.

### C. L-infinity Norm Approximation

The L-infinity norm approximates the magnitude of complex signals by taking the maximum value between the absolutes of the real and imaginary components. It's a simple and efficient algorithm that requires minimal hardware. However, the simplicity comes at the cost of poor accuracy.

## IV. State-of-the-Arts PLV/PAC Extraction Units

The PLV/PAC feature extraction units have been proposed in various implementations. Most of the implementations utilizes the filter-Hilbert method for complex signal extraction processes. However, the features computation is done differently, either using CORDIC processors or LPE with trigonometric LUT and L-infinity norm approximation. This section presents an overview on the state-of-the-art PLV/PAC extraction units.

In [1], a PLV extraction unit using CORDIC processors was presented. The input signals are band-limited and passed through a Hilbert filter in parallel with an all-pass filter to extract the complex signals and compensate for the Hilbert block delay. The PLV feature is then computed using three CORDIC processor cores and two moving average FIR filters, as shown in Fig.3. The phases of two input complex signals are extracted by the first CORDIC core. The subtractor computes the phase difference, which is used by the second CORDIC core to obtain sine and cosine values. Two moving average FIR filters performs the averaging over a sliding time window of length N. The third CORDIC core gets the final magnitude of the PLV feature. The first CORDIC core also extracts the magnitudes of the input signals as extra features. However, using only the PLV feature is more efficient for seizure detection.

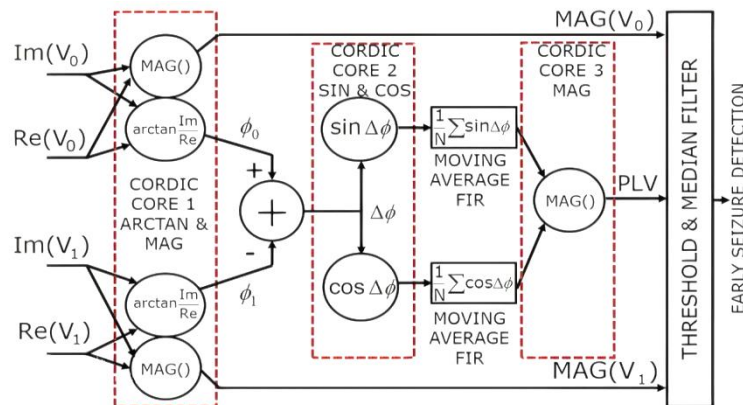


Figure 3: The PLV CORDIC-based computation unit suggested in [9].

In [11], a single PLV/PAC extraction unit is implemented by considering the similarity between the PLV and PAC formulas. Complex signal extraction is achieved using filter-Hilbert method with shared multipliers and adders to enhance power and area efficiencies. However, a memory is required to store the coefficients for each band. CORDIC processors are used for PLV/PAC computations and IIR filters are utilized for averaging, reducing power consumption and area.

In [12, 13], PLV feature was calculated using coarse approximation methods without extracting phase information. The methods are based on measuring the time periods between two consecutive minima of the two input signals. However, they suffer from inaccuracy and cannot extract the PAC feature.

A PLV/PAC extraction unit had been suggested in [14] and re-used in [15, 16]. Complex signals are extracted using filter-Hilbert method with sharing resources. PLV and PAC computation unit is implemented using an LPE, trigonometric LUT, and L-infinity norm - see Fig.4.

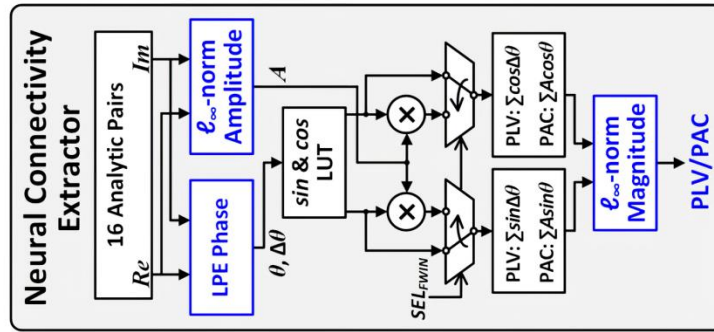


Figure 4: The PLV/PAC Computation Unit Suggested in [14].

At first, the PAC magnitude modulated complex signals are applied to an L-infinity norm block to extract the magnitude value. The PAC phase modulating complex signals as well as the PLV two input complex signals, are applied to a shared LPE. A subtractor gets the phase difference between for the PLV. After that, a trigonometric LUT is utilized to obtain the corresponding sine and cosine values. Accumulators and shifters are used to perform the averaging over the time window. The final values for PLV and PAC are computed using an L-infinity norm block. This implementation significantly reduces power and area consumptions at negligible accuracy loss.

**V. Limitations**

As previously mentioned, extracting PLV and PAC features involves two main steps: extracting the complex signals within the bands of interest, and performing the PLV and PAC computation. The extraction process of complex signals can be achieved through the Morlet wavelet convolution or a band-pass filter followed by the Hilbert transform. The filter-Hilbert method is the technique conventionally used for on-chip feature extraction. However, high numbers of filter taps, coefficients, and multipliers are still needed. Resource sharing reduces the power and area; however, it requires memory to store coefficients for different bands. For the features computation, CORDIC processors achieve high accuracy at the cost of high power and area. Hence, the CORDIC-based approach is unsuitable for high channel count implantable devices. Instead, an LPE with Trigonometric LUTs and L-infinity norm achieve significant power and area reduction at a negligible accuracy loss. However, two steps are used to obtain the sine and cosine functions for PAC and PLV. First, the LPE approximates the phase. Then, a trigonometric LUT extracts the sine and cosine values. Table 1 illustrates a comparison between different PAC/PLV unit.

Table 1: Comparison Between Techniques:

Parameter	JSSC'13 [10]	TBioCAS'19 [13]	CICC'22 [15]	ISSCC'18 [11]	ISCAS'2023 [25]
Supply Voltage (V)	1.2	0.5	0.85	1.2	1.2
Process (nm)	130	180	65	130	40
PLV/PAC channels	32 PLV	1 PLV	8 PAC/PLV	65 AC/PLV	16 AC/PLV
Total Power (µW)	400	0.015	9.7	200.4	3.2
Power/ch (µW)	12.5	0.015	1.2	3.1	0.2
Area (mm <sup>2</sup> )	0.632	0.025	0.033	0.245	0.005

In summary, the previously suggested PLV/PAC extraction units in the state-of-the-art exhibit two significant limitations. Firstly, the complex signal extractor requires large numbers of filter taps that lead to a high number of

coefficients and multipliers. Secondly, the computation of sine and cosine functions is a two-step process, resulting in a complex calculation for feature computation.

## VI. Conclusion

Neural interfaces shows promise in treating neurological conditions. To enable fully implantable treating interfaces, efficient oscillatory feature extraction units are required. Extracting oscillatory synchronization features such as PLV and PAC involves two main blocks. The first block is a complex signal extractor that extracts complex signal representations within the frequency bands of interest. The second block for extracting the synchronization features is a PLV/PAC computation unit that calculates the PLV and PAC features from the extracted complex signals. For implementing the PLV/PAC computation unit, CORDIC processors or LPE with trigonometric LUT and L-infinity norm approximation can be used. The LPE-based method is more efficient in terms of power and area compared to the CORDIC-based one. However, this LPE-based method requires a two-step computation for the sine and cosine functions needed to compute the PLV and PAC.

This article explores different techniques suggested for extracting the PLV and PAC features. Additionally, the article provides an overview of the current state-of-the-art units and their limitations.

## VII. References

- [1] O. Alshaltone, R. Shaikh, N. Nasir, F. Barneih, M. Sameer, T. Bonny, M. A. Shabi, and A. A. Shammaa, "Epileptic seizure detection using short time fourier transform and convolutional neural network," in *The 3rd International Conference on Distributed Sensing and Intelligent Systems (ICDSIS 2022)*, vol. 2022, 2022, pp. 103-112.
- [2] K. W. Scangos, A. N. Khambhati, P. M. Daly, G. S. Makhoul, L. P. Sugrue, H. Zamanian, T. X. Liu, V. R. Rao, K. K. Sellers, H. E. Dawes et al., "Closed-loop neuromodulation in an individual with treatment-resistant depression," *Nature medicine*, vol. 27, no. 10, pp. 1696-1700, 2021.
- [3] T. Denison and M. J. Morrell, "Neuromodulation in 2035: the neurology future forecasting series," *Neurology*, vol. 98, no. 2, pp. 65-72, 2022.
- [4] M. P. Branco, S. H. Geukes, E. J. Aarnoutse, N. F. Ramsey, and M. J. Vansteensel, "Nine decades of electrocorticography: A comparison between epidural and subdural recordings," *European Journal of Neuroscience*, vol. 57, no. 8, pp. 1260-1288, 2023.
- [5] Y. Zhang, N. Mirchandani, S. Abdelfattah, M. Onabajo, and A. Shrivastava, "An ultra-low power rssi amplifier for eeg feature extraction to detect seizures," *IEEE Transactions on Circuits and Systems II: Express Briefs*, vol. 69, no. 2, pp. 329-333, 2021.
- [6] N. E. C ́ ampora, C. J. Mininni, S. Kochen, and S. E. Lew, "Seizure localization using preictal phase-amplitude coupling in intracranial electroencephalography," *Scientific Reports*, vol. 9, no. 1, p. 20022, 2019.
- [7] K. Abdelhalim, H. M. Jafari, L. Kokarovtseva, J. L. P. Velazquez, and R. Genov, "64-channel UWB wireless neural vector analyzer SOC with a Closed-Loop phase Synchrony-Triggered neurostimulator," *IEEE J. Solid-State Circuits*, vol. 48, no. 10, pp. 2494-2510, Oct. 2013.
- [8] H. Yassin, A. Akhoundi, E. -S. Hasaneen and D. G. Muratore, " A Low-Power Oscillatory Feature Extraction Unit for Implantable Neural Interfaces," *2023 IEEE International Symposium on Circuits and Systems (ISCAS)*, Monterey, CA, USA, 2023.
- [9] K. Abdelhalim, V. Smolyakov, and R. Genov, "Phase-synchronization early epileptic seizure detector vlsi architecture," *IEEE transactions on biomedical circuits and systems*, vol. 5, no. 5, pp. 430-438, 2011.
- [10] K. Abdelhalim, H. M. Jafari, L. Kokarovtseva, J. L. P. Velazquez, and R. Genov, "64- channel uwb wireless neural vector analyzer soc with a closed-loop phase synchronytriggered neurostimulator," *IEEE Journal of Solid-State Circuits*, vol. 48, no. 10, pp. 2494- 2510, 2013.
- [11] G. O'Leary, D. M. Groppe, T. A. Valiante, N. Verma, and R. Genov, "Nurip: Neural interface processor for brain-state classification and programmable-waveform neurostimulation," *IEEE Journal of Solid-State Circuits*, vol. 53, no. 11, pp. 3150-3162, 2018.
- [12] S. Davila-Montero and A. J. Mason, "An in-situ phase-preserving data decimation method ´ for high-channel-count wireless mecg arrays," in *2017 IEEE Biomedical Circuits and Systems Conference (BioCAS)*. IEEE, 2017, pp. 1-4.

- [13] M. Delgado-Restituto, J. B. Romaine, and A. Rodríguez-Vázquez, "Phase synchronization operator for on-chip brain functional connectivity computation," *IEEE Transactions on Biomedical Circuits and Systems*, vol. 13, no. 5, pp. 957–970, 2019.
- [14] U. Shin, C. Ding, L. Somappa, V. Woods, A. S. Widge, and M. Shoaran, "A 16-channel 60 $\mu$ w neural synchrony processor for multi-mode phase-locked neurostimulation," in *2022 IEEE Custom Integrated Circuits Conference (CICC)*, 2022, pp. 01–02.
- [15] U. Shin, C. Ding, B. Zhu, Y. Vyza, A. Trouillet, E. C. M. Revol, S. P. Lacour, and M. Shoaran, "Neuraltree: A 256-channel 0.227- $\mu$ j/class versatile neural activity classification and closed-loop neuromodulation soc," *IEEE Journal of Solid-State Circuits*, vol. 57, no. 11, pp. 3243–3257, 2022.
- [16] U. Shin, C. Ding, V. Woods, A. S. Widge, and M. Shoaran, "A 16-channel low-power neural connectivity extraction and phase-locked deep brain stimulation soc," *IEEE Solid State Circuits Letters*, vol. 6, pp. 21–24, 2023.
- [17] C. M. Akujuobi, *Wavelets and wavelet transform systems and their applications*. Springer, 2022.
- [18] Z. He, X. Xing, X. Zheng, H. Feng, H. Fu, and G. Gielen, "Low power and high speed designs of cic filter for sigma-delta adcs," in *2022 IEEE Asia Pacific Conference on Circuits and Systems (APCCAS)*. IEEE, 2022, pp. 236–240.
- [19] M. X. Cohen, *Analyzing neural time series data: theory and practice*. MIT press, 2014.
- [20] S. Scholl, "Fourier, gabor, morlet or wigner: Comparison of time-frequency transforms. arxiv 2021," arXiv preprint arXiv:2101.06707.
- [21] A. Zabidi, W. Mansor, Y. K. Lee, and C. W. N. F. Che Wan Fadzal, "Short-time fourier transform analysis of eeg signal generated during imagined writing," in *2012 International Conference on System Engineering and Technology (ICSET)*, 2012, pp. 1–4.
- [22] M. Rhif, A. Ben Abbes, I. R. Farah, B. Martínez, and Y. Sang, "Wavelet transform application for/in non-stationary time-series analysis: A review," *Applied Sciences*, vol. 9, no. 7, p. 1345, 2019.
- [23] C. M. Akujuobi, *Wavelets and wavelet transform systems and their applications*. Springer, 2022.
- [24] M. X. Cohen, "A better way to define and describe morlet wavelets for time-frequency analysis," *NeuroImage*, vol. 199, pp. 81–86, 2019.
- [25] S. Morales and M. E. Bowers, "Time-frequency analysis methods and their application in developmental eeg data," *Developmental cognitive neuroscience*, vol. 54, p. 101067, 2022.